Journal of Organometallic Chemistry 706-707 (2012) 37–45

Contents lists available at SciVerse ScienceDirect

Journal of Organometallic Chemistry

journal homepage: www.elsevier.com/locate/jorganchem

Synthesis, crystal structure and electrocatalysis of 1,2-ene dithiolate bridged diiron carbonyl complexes in relevance to the active site of [FeFe]-hydrogenases

Gummadi Durgaprasad, Ramababu Bolligarla, Samar K. Das*

School of Chemistry, University of Hyderabad, Hyderabad 500046, Andhra Pradesh, India

ARTICLE INFO

Article history:
Received 5 November 2011
Received in revised form
16 January 2012
Accepted 17 January 2012

Keywords:
[FeFe]hydrogenase
1,2-ene dithiolate bridged diiron carbonyl complex
Bioinorganic chemistry
e^-- withdrawing effect
Electrochemistry

ABSTRACT

A series of binuclear Fe^IFe^I complexes have been prepared by the treatment of *N*–heterocyclic 1,2-dithiols, such as, quinoxaline-6,7-dithiol ($H_2$6,7-qdt), 2,3-diphenyl-6,7-quinoxaline dithiol (H_2diph-6,7-qdt) and 2,1,3-benzothiadiazole-5,6-dithiol (H_2btdt) with $Fe_2(CO)_9$ resulting in the formation of [Fe_2\{μ-6,7-qdt\}$(CO)_6$] (**1**), [Fe_2\{μ-diph-6,7-qdt\}$(CO)_6$] (**2**) and [Fe_2\{μ-btdt\}$(CO)_6$] (**3**) respectively, that serve as model systems for the active site of [FeFe]-hydrogenase. These new complexes **1**–**3** have been characterized by IR, ^{1}H, ^{13}C, and ^{31}P\{^{1}H\} NMR, mass spectroscopy, elemental analysis and single-crystal X-ray structure analysis. The electrochemistry of **1**–**3** was performed by cyclic voltammetry and the electrocatalytic activities of model complexes **2** and **3** toward proton reduction of a strong acid *p*–HOTs have been described.

1. Introduction

The [FeFe] hydrogenases are vital enzymes, which are well known to catalyze the reduction of protons to molecular hydrogen in numerous metallo-enzyme systems with extremely high efficiency which is, therefore, of great interest in the field of renewable energies [1–3]. [FeFe]-hydrogenases, isolated from *Desulfovibrio desulfuricans* and *Clostridium pasteurianum* [4,5], feature a butterfly 2Fe2S subunit with CO and CN^- ligands with one of the Fe (Fe_p) atoms linked to a 4Fe4S cluster by the sulfur atom of a cysteinyl ligand (Fig. 1(i)). Eventually, such a structure has inspired the organometallic chemists to do an extensive work on developing simple and robust structural analogues to mimic the [FeFe]-hydrogenase active site. Several review articles have been published in recent times that are associated with hydrogenase model complexes and their catalytic activities [6–10]. The catalytic property for the hydrogen generation, mediated by [FeFe]H_2ase model complexes, can be tuned by the substitution of the CO ligands of diiron carbonyl complexes. Thus, displacement of one or two CO ligands from [FeFe]H_2ase model complexes by various good ligands such as CN^-, phosphine, phosphite, and carbene has been reported [11–19]. These carbonyl substituted complexes also serve as synthetic models of the active site of [FeFe]H_2ases. To date, a large number of biomimetic models for the active site of [FeFe] hydrogenase has been prepared and structurally characterized [20–26]. Among such models, we are particularly interested in 1,2-ethylene-dithiol bridged 2Fe2S core, such as, benzene dithiolate (bdt^{2-}) bridged diiron core (representation **A**, shown below in Fig. 1(ii)) type models [27–30].

Capon and co-workers first reported the compound **A** as [FeFe]-hydrogenase active site model system [31] and further Lichtenberger, Evans, Glass and their co-workers have successfully demonstrated electrocatalytic hydrogen generation from weak acid (HOAc) by using the same system **A**. They proposed a novel mechanism, deduced from both electrochemical and theoretical studies on complex **A** [32,33]. Sascha Ott and his co-workers worked on arene dithiolate bridged diiron complexes extensively [34–38]. For the system **A**, the benzene dithiolate (bdt^{2-}) ligand has a special ability; it assists to modulate the redox reactions of the catalyst by lowering the potential difference between the successive reduction states. This has been explained by an interaction of the metal d-orbitals with a combination of the filled sulfur p_π orbitals and the arene p_π orbitals, which acts to shield the change in electron density at the iron center as the oxidation state is changed, thus minimizing the changes in electron energies upon reduction. The importance of 1,2-ethylene-dithiolate in such model complexes can also be realized by the fact that “Nature” has used this ligand in the active site of Mo/W-oxotransferase redox enzymes because of its unique electronic property [39,40].

* Corresponding author.
E-mail address: skdsc@uohyd.ernet.in (S.K. Das).

0022-328X/$ – see front matter © 2012 Elsevier B.V. All rights reserved.
doi:10.1016/j.jorganchem.2012.01.021

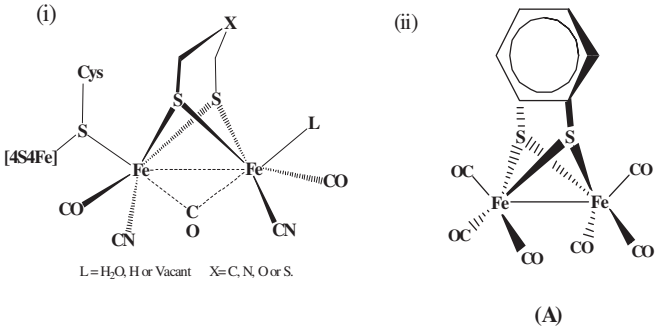

Fig. 1. (i) Schematic view of the active site of [FeFe]hydrogenase. (ii) **A** represents benzene dithiol bridged diiron complex as a model of [FeFe] hydrogenase active site.

Thus, the rational design and syntheses of 1,2-ethylene-dithiolate-coordinated 2Fe2S complexes are challenging tasks for synthetic chemists in modeling the active sites of [FeFe]H_2ases. In view of this, recently we have reported pyrazine dithiolate bridged diiron complexes as [FeFe]hydrogenase active site model complexes [41]. In the present contribution, we preferred and synthesized the following *N*–heterocyclic ene-1,2-dithiol (benzene ring attached *o*-dithiols) ligands, such as, quinoxaline-6,7-dithiol ($H_2$6,7-qdt), 2,3-diphenyl-6,7-quinoxaline dithiol (H_2diph-6,7-qdt) and 2,1,3-benzothiadiazole-5,6-dithiol (H_2btdt) as shown in Scheme 1.

We have synthesized model complexes [Fe_2(μ-6,7-qdt)$(CO)_6$] (**1**), [Fe_2(μ-diph-6,7-qdt)$(CO)_6$] (**2**) and [Fe_2(μ-btdt)$(CO)_6$] (**3**) using these *N*-heterocyclic 1,2-dithiol ligands (Scheme 1). Here we describe the syntheses, spectroscopic characterization, X-ray crystallography and electrochemical studies of complexes **1**–**3**. We have demonstrated the electrocatalytic proton reduction of a strong acid *p*–HOTs mediated by compounds **2** and **3** and plausible catalytic mechanisms for the production of molecular hydrogen have been proposed.

2. Results and discussion

2.1. Synthesis and characterization of N–heterocyclic 1,2-dithiol ligands

$H_2$6,7-qdt. $H_2$6,7-qdt was prepared by literature procedure [42].

H_2diph-6,7-qdt. The starting precursor for this synthesis is 4,5-bis(thiocyanato)-benzene-1,2-diamine, which was prepared from benzene-1,2-diamine and KSCN/Br_2 by following reported literature procedure [43]. 2,3-Diphenyl-6,7-bis-thiocyanato-quinoxaline (**B**) (see Scheme below) was prepared according to modified literature procedure [44,45], which was obtained by a condensation reaction between the 4,5-bis(thiocyanato)-benzene-1,2-diamine and benzil by using iodine as a catalyst in acetonitrile solution at room temperature for 1 h affording a quantitative yield. Finally H_2diph-6,7-qdt was synthesized by treating compound **B** with Na_2S followed by acidification, which gives a good yield (90%) as shown in Scheme 2. Compound **B** and ligand H_2diph-6,7-qdt were characterized by regular IR, NMR, LC-MS spectral and elemental analysis.

H_2btdt. H_2btdt was synthesized by a reported literature procedure [43].

2.2. Synthesis and characterization of model complexes [Fe_2(μ-6,7-qdt)$(CO)_6$] (**1**), [Fe_2(μ-diph-6,7-qdt)$(CO)_6$] (**2**) and [Fe_2(μ-btdt)$(CO)_6$] (**3**)

We have synthesized [FeFe]-hydrogenase model compounds [Fe_2(μ-6,7-qdt)$(CO)_6$] **(1)**, [Fe_2(μ-diph-6,7-qdt)$(CO)_6$] **(2)** and [Fe_2(μ-btdt)$(CO)_6$] **(3)** by treating 6,7-quinoxaline-dithiol ($H_2$6,7-qdt), diphenyl-6,7-quinoxaline dithiol (H_2diph-6,7-qdt) and 2,1,3-benzothiadiazole-5,6-dithiol (H_2btdt) respectively with $Fe_2(CO)_9$ in THF at 50 °C as shown in Scheme 3. Complexes **1, 2** and **3** are air stable red solids and purified directly by column chromatography, which have been fully characterized by IR, ^{1}H, and ^{13}C NMR spectroscopy and elemental analysis. The IR spectra of complexes **1, 2** and **3** show four to five strong absorption bands in the region of 2080–1950 cm^{-1}, that are assigned to the terminal carbonyl groups. The ^{1}H NMR spectrum (in $CDCl_3$ solution at 298 K) of complex **1** displays two singlets at δ 8.66 and 7.86 ppm. Compound **2** shows one singlet at δ 7.94 and one multiplet for two phenyl groups at δ 7.43–7.29 ppm whereas for compound **3**, only one singlet at δ 7.85 ppm is observed in their respective NMR spectra. The ^{13}C NMR spectra of complexes **1**, **2** and **3** exhibit only one peak at δ 207 ppm for their terminal carbonyl group.

The molecular structures of **1**, **2** and **3** are unambiguously confirmed by X-ray diffraction technique and thermal ellipsoidal plots are shown in Fig. 2a–c. Table 1 lists their selected bond lengths and bond angles. The wine-red colored crystals of complexes **1**, **2** and **3** are grown by cooling respective CH_2Cl_2 solutions at −10 °C. The crystal structure analyses show that the complexes **1**, **2** and **3** crystallize in monoclinic space groups $P2_1/c$, $C2/c$ and $P2_1/c$ respectively. $Z' = 1$ for complexes **1**, **2** and **3** and bonding dimensions within the complexes are unexceptional as shown in Fig. 2. The central 2Fe2S structures of all three diiron 1,2-ene dithiolate bridged complexes (**1**, **2** and **3**) are in the butterfly conformation and each iron atom is coordinated with a pseudo square–pyramidal geometry as in previously reported relevant models [11,17,46–50]. In addition, the Fe···Fe separation in the crystal structures of complexes **1**, **2** and **3** are 2.4900, 2.5023 and 2.4907 Å respectively, that are somewhat longer than that of complex **A** (2.480(2) Å) (Fig. 1) [28] and relatively shorter than

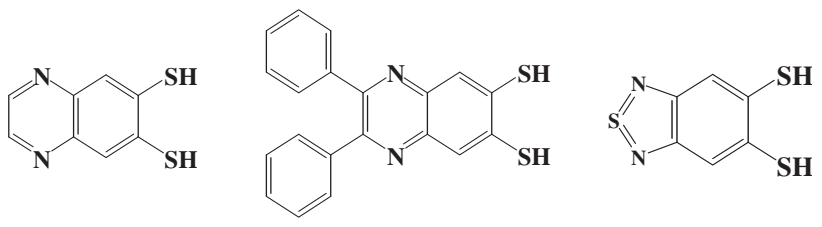

$H_2$6,7-qdt H_2diph-6,7-qdt H_2btdt

Scheme 1. *N*–heterocyclic 1,2-dithiol ligands.

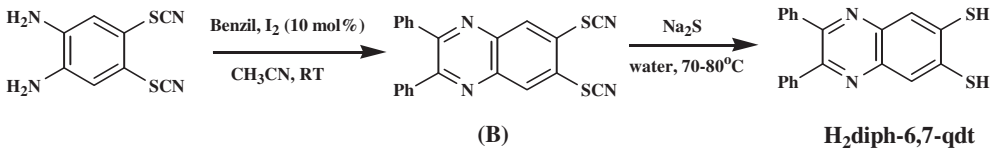

Scheme 2. Synthetic route of H_2diph-6,7-qdt.

those found in *D. desulfuricans* [5] and *Clostridium pasteurianum* [4] (*ca*. 2.6 Å).

Interestingly, complex **3** shows non-covalent interactions, such as, weak S···N and S···S supramolecular contacts. The S···N contact distance is 3.0701(1), which is less than the sum of their van-der Waals radii (1.55 Å for nitrogen and 1.80 Å for sulphur) [51]. The non-covalent S···S interactions are described by a distance of 3.641(1) Å. These combined weak S···N and S···S non-covalent interactions result in the formation of one dimensional chainlike arrangement as shown in Fig. 2d.

2.3. Electrochemistry of model complexes *1*–*3*

The electrochemical properties of complexes **1**–**3** were investigated by cyclic voltammetry (CV) studies in MeCN (with 0.1 M n–Bu_4NClO_4 as supporting electrolyte, $\nu = 0.1$ V/s) solution under an atmosphere of Ar. Table 2 lists the electrochemical data and Fig. 3 shows the cyclic voltammograms of the complexes **1**–**3**. They were initiated from the open circuit and scanned in the cathodic direction as indicated in Fig. 3. It is shown that complexes **1**, **2** and **3** display one quasi–reversible two electron reduction process at $E_{1/2} = -1.23$, -1.24 and -1.25 V (*vs*. Fc/Fc^+) respectively, as shown in Fig. 3. The electrochemical behavior of the complex **A** (Fig. 1 (ii)) was already well–established and it shows that the first reduction potential undergoes a two-electron process that occurs at $E_{1/2} = -1.27$ V [32,34,52]. This reflects that the present ligand system *N*–heterocyclic 1,2-ene dithiolates (Scheme 1) is of more electron-withdrawing character than benzene dithiolate (bdt^{2-}) in complex **A**, thereby, shifting the reduction potentials of complexes **1**, **2** and **3** to relatively more anodic side by 40, 30 and 20 mV, respectively (see Table 2) than complex **A** with benzene dithiolate (bdt^{2-}) ligand. As a consequence, complexes **1**, **2** and **3** are thermodynamically more facile than that of complex **A** as far as reduction is concerned. The reduction potential of the related model compound, quinoxaline 2,3-dithiol (H_2qdt) bridged diiron complex [$Fe_2\{\mu$-qdt$\}(CO)_6$], is comparable ($E_{1/2} = -1.22$ V) [34,41] to those of complexes **1**, **2** and **3**. In all these cases, the electron-withdrawing nature of the ligands decreases the electron density around the iron centers, making the reduction process easier [34].

2.4. Electrocatalytic hydrogen formation from p-toluenesulfonic acid (p-HOTs) by complexes *2* and *3*

The behavior of electrocatalytic proton reductions by compounds **2** and **3** were performed by cyclic voltammograms in the presence of a strong acid *p*-toluenesulfonic acid (*p*-HOTs). The $Eo_{p\text{-HOTs}}$ for *p*-HOTs is -0.65 V *vs*. Fc/Fc^+ in acetonitrile [53]. This indicates that the least negative potential of the catalyst, that will allow reduction of *p*-HOTs to dihydrogen, should be more negative

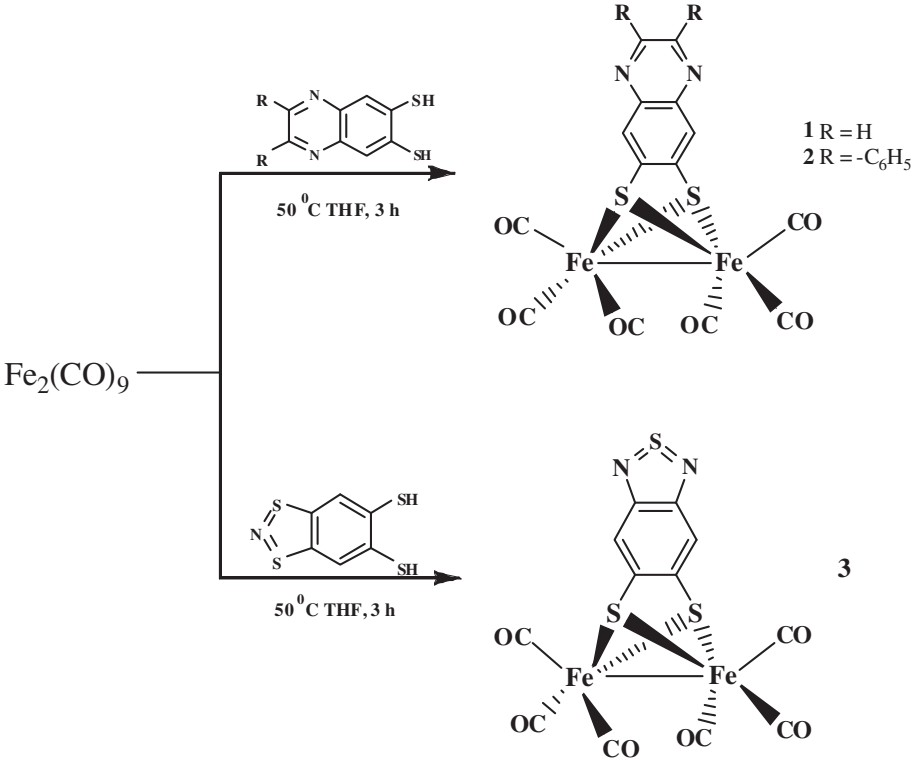

Scheme 3. Synthesis of complexes **1**–**3**.

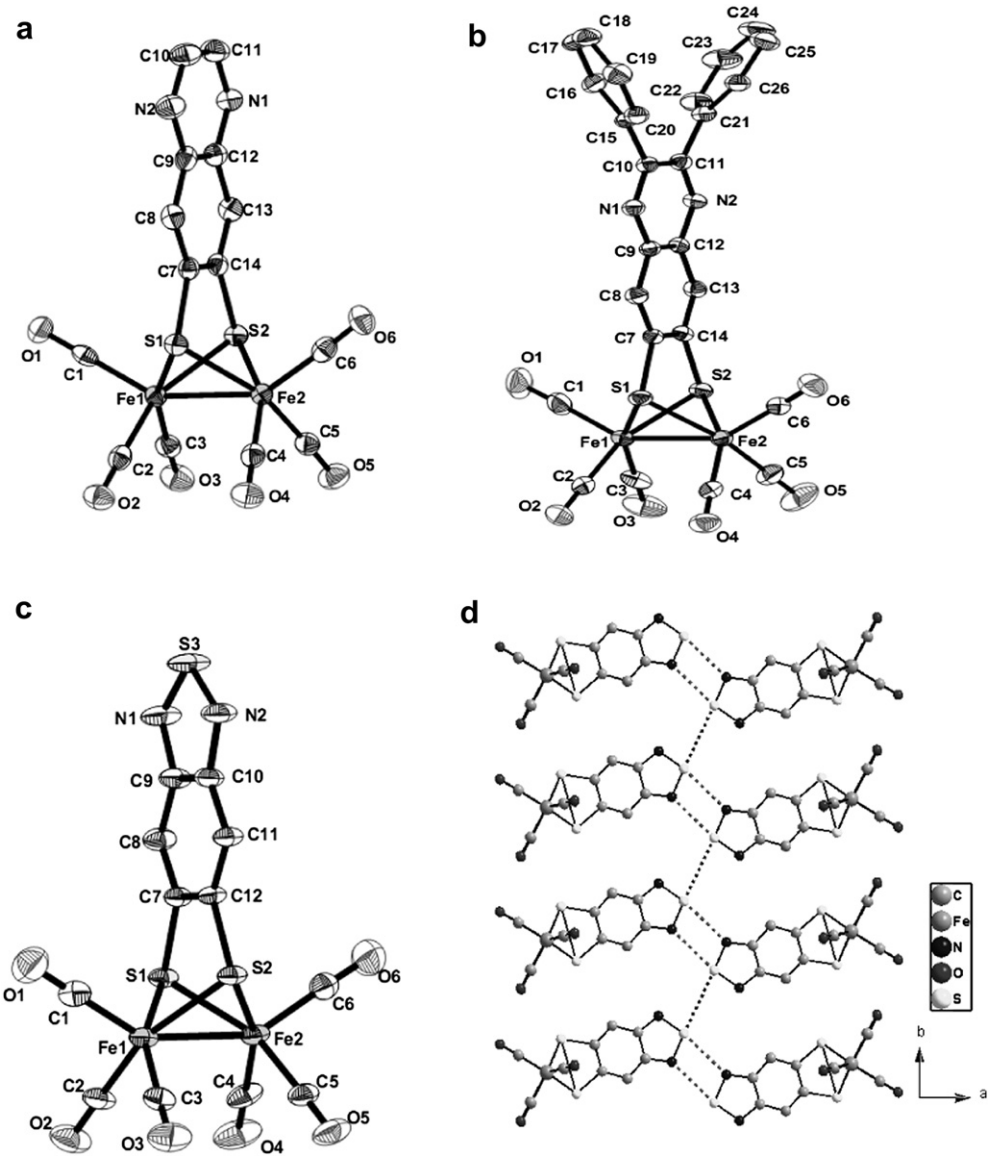

Fig. 2. Molecular structures of compounds (a) **1**, (b) **2** and (c) **3** with thermal ellipsoids at 50% probability. Hydrogen atoms are omitted for clarity. (d) The molecular packing diagram of compound **3**, characterized by N···S and S···S weak interactions, when viewed down to the crystallographic *c* axis.

Table 1
Selected bond lengths [Å] and angles [°] for complexes **1**, **2** and **3**.

	1	2	3
Fe(1)–S(1)	2.2658 (7)	2.2632 (16)	2.267 (2)
Fe(2)–Fe(1)	2.4740 (5)	2.4772 (11)	2.4907 (18)
O(1)–C(1)	1.136 (3)	1.128 (8)	1.147 (9)
C(9)–N(1)	1.366 (3)	1.359 (6)	1.357 (8)
Fe(1)–C(1)	1.807 (3)	1.801 (7)	1.785 (9)
S(1)–Fe(1)–Fe(2)	56.96 (2)	56.96 (4)	56.52 (6)
S(2)–Fe(1)–Fe(2)	56.819 (19)	56.56 (4)	56.60 (6)
Fe(1)–S(1)–Fe(2)	66.15 (2)	66.28 (4)	66.73 (6)

Table 2
Cyclic voltammetric data (*vs*. Fc/Fc^{+}) for complexes **1**–**3** in MeCN[a].

	1	2	3
E^{1}_{pc}(V)	−1.34	−1.34	−1.35
E^{1}_{pa}(V)	−1.12	−1.13	−1.15
$E^{red}_{1/2}$(V)	−1.23	−1.24	−1.25

[a] 0.1 M *n*-Bu_4NClO_4 in CH_3CN; scan rate 100 mV s^{-1}; working electrode: glassy carbon electrode of diameter 3 mm; reference electrode: non-aqueous Ag/Ag^{+} electrode (0.01 M $AgNO_3$ in CH_3CN); counter electrode: platinum wire.

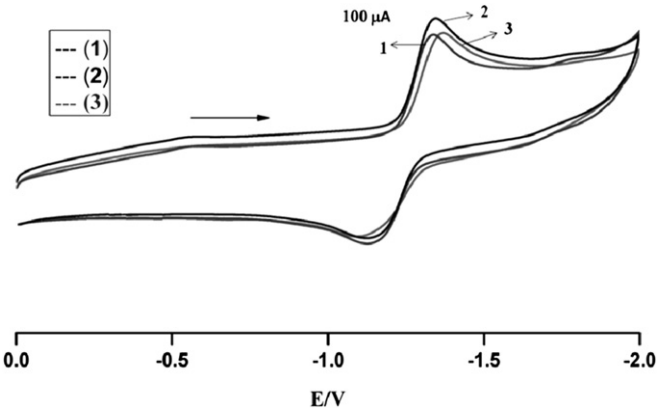

Fig. 3. Cyclic voltammograms of complexes **1**, **2** and **3** (1.0 mM) in 0.1 M *n*-Bu_4NClO_4/MeCN at a scan rate of 100 mV s^{-1}. Potential are *vs*. Fc/Fc^{+}.

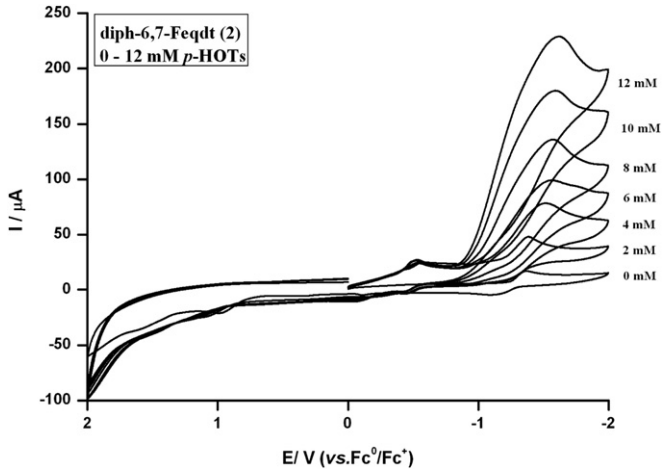

Fig. 4. Cyclic voltammogram of complex **2** with 1.0 mM complex and 0–12 mM *p*-HOTs in CH_3CN solution (0.1 M n-Bu_4NClO_4) at a scan rate of 100 mV s^{-1}.

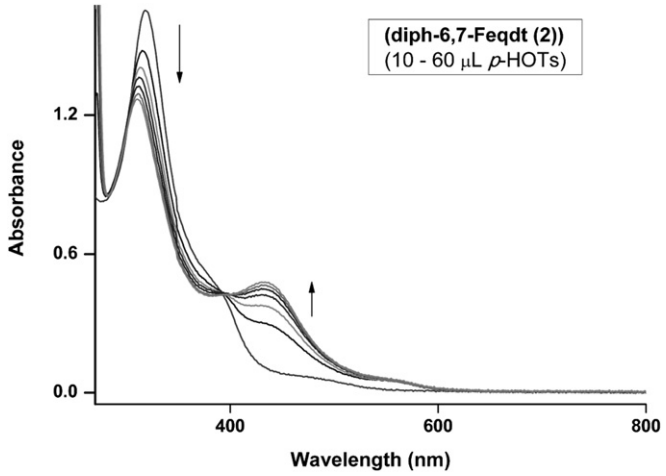

Fig. 5. Changes in the absorption spectra of compound **2,** (5.0×10^{-5} M) upon the addition of 10–60 μL aliquots of dilute *p*–HOTs (0.1 mM) in CH_3CN.

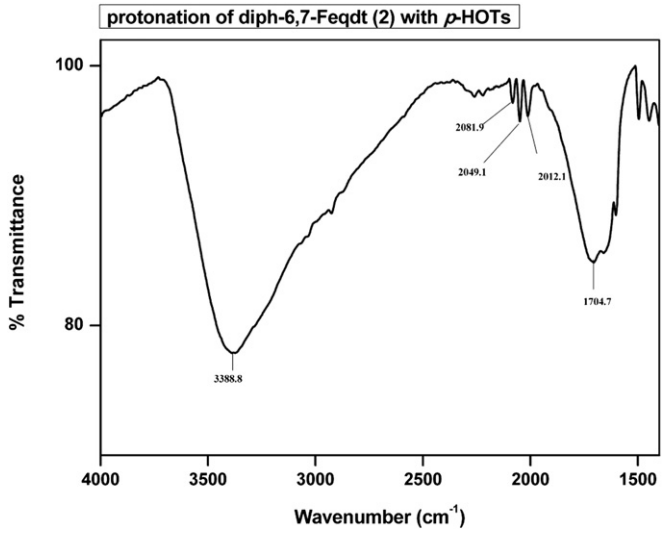

Fig. 6. FTIR spectrum of acetonitrile solution of compound **2** treated with *p*–HOTs. 5 mg of *p*-HOTs was added to a CH_3CN solution (2 mL) of complex **2** (10 mg).

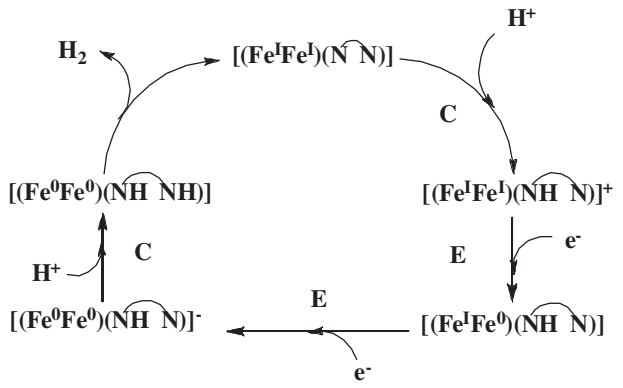

Fig. 7. A schematic representation of plausible CEEC mechanism for electrocatalytic proton reduction in the presence of *p*–HOTs for compound **2**.

than −0.65 V *vs*. Fc/Fc^+. As described in preceding section, the E values obtained from the electrochemical reductive responses of compounds **2** and **3** qualify the requirement of reducing *p*-HOTs to dihydrogen. For compound $[Fe_2\{\mu\text{-diph-6,7-qdt}\}(CO)_6]$ (**2**), upon the addition of 2 mmol of *p*-HOTs, a new peak appeared at $E_{pc} = -0.53$ V and the current intensity of the reduction at $E_{pc} = -1.35$ V increased with a cathodic shift by 40 mV. The height of this reduction peak at $E_{pc} = -1.35$ V continuously grew as the acid concentrations increase from 2 to 12 mM with final cathodic shift by 260 mV (Fig. 4). On the other hand, the current intensity of the anodic shifted peak $E_{pc} = -0.53$ V (appeared on addition of 2 mmol of *p*-HOTs) did not grow up further with sequential increments of the acid concentrations (4–12 mM). This observation indicates the protonation of one of the ring nitrogens present in the ligand system of compound **2**. This is supported by electronic absorption spectral changes, occurred on addition of 10–60 μL *p*-HOTs to the acetonitrile solution of complex **2** that shows a clean isosbestic point at 395 nm (Fig. 5). Protonation of the ring nitrogens in the complex **2** is also observed on energies of the IR bands as shown in the FTIR spectrum (Fig. 6) of compound **2** solution (CH_3CN) treated with *p*-HOTs. As shown in Fig. 6, the IR spectrum exhibited significant changes in the carbonyl region. When protonation occurs, there is a considerable shift of the CO bands to higher frequencies (energy) region. The IR peaks at 2076, 2037, 2028, 2003, 1973 cm^{-1} (compound **2**) shift to 2081,

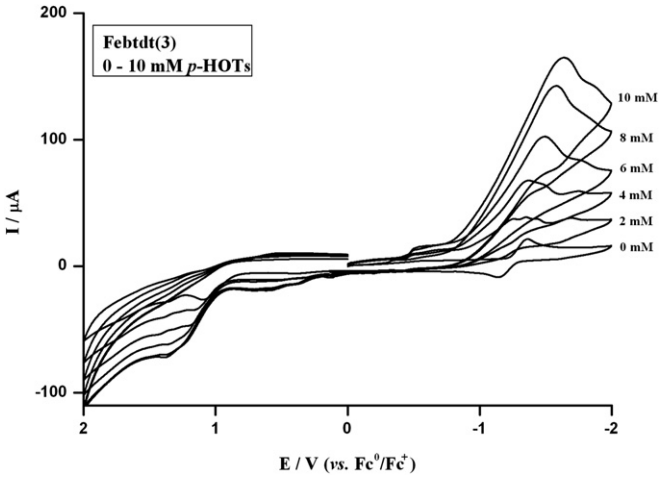

Fig. 8. Cyclic voltammogram of complex **3** with 1.0 mM complex and 0–10 mM *p*-HOTs in CH_3CN solution (0.1 M n-Bu_4NClO_4) at a scan rate of 100 mV s^{-1}.

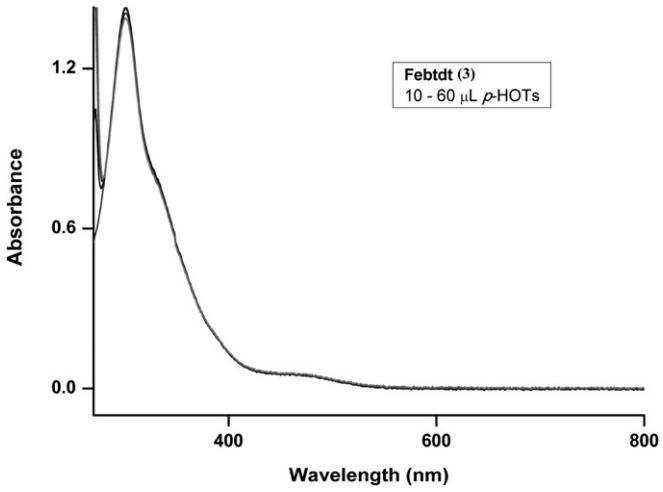

Fig. 9. Changes in the absorption spectra of compound **3,** (5.0×10^{-5} M) upon the addition of 10–60 μL aliquots of dilute *p*–HOTs (0.1 mM) in CH_3CN.

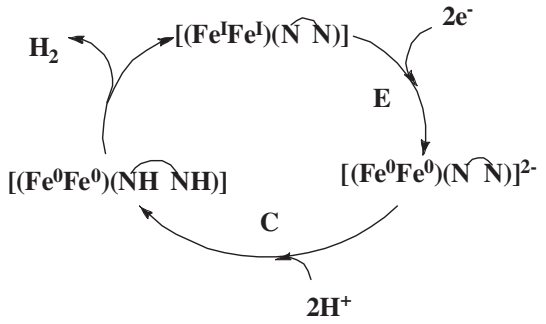

Fig. 10. A schematic representation of plausible EC mechanism for electrocatalytic proton reduction in the presence of *p*–HOTs for compound **3**.

2049, 2012 cm^{-1} on protonation. The N–H bond, formed on protonation, displays a strong and broad absorption band at 3388 cm^{-1} region because of N–H stretching vibrations (Fig. 6). For comparison, the solution IR spectrum of compound **2** (without adding *p*-HOTs) is shown in the last section of Supporting Information.

The continuous growth of the reduction peak at $E_{pc} = -1.35$ V with final cathodic shift of 260 mV (on addition of 2–12 mM *p*-HOTs) is characteristic of an electrochemical catalytic reduction of *p*-HOTs to hydrogen. The catalyzed reduction of *p*-HOTs occurs at about −1.61 V *vs.* Fc/Fc^+ with overpotential of 0.96 V. The cyclic voltammograms (Fig. 4) and the spectroscopic evidences (Figs. 5 and 6) suggest a CEEC (chemical-electrochemical-electrochemical-chemical) mechanism (Fig. 7) for the electrocatalytic proton reduction by diph-6,7-qdt-bridged all-carbonyl $\{Fe^1Fe^1\}$ compound **2**. A possible CECE (chemical-electrochemical-chemical-electrochemical) mechanism can be ruled out by the fact that the catalyzed reduction of *p*-HOTs occurs (present study) with cathodic shift instead of anodic shift; earlier report of the ADT-diiron complex $[\{(\mu\text{-}SCH_2)_2N(4\text{–}NO_2C_6H_4)Fe_2(CO)_6]$ catalyzed acid reduction has been described by a CECE mechanism, for which the catalyzed acid reduction occurs with an anodic shift [54].

The hexa carbonyl compound $[Fe_2\{\mu\text{-btdt}\}(CO)_6]$ (**3**) exhibits the electrocatalytic proton reduction with *p*-HOTs as shown in Fig. 8. In this case, protonation of oxidized $\{Fe^IFe^I\}$ species does not occur as shown by electronic absorption spectral scans, recorded on addition of 10–60 μL *p*-HOTs to the acetonitrile solution of complex **3** that do not show any spectral changes (Fig. 9). The current height of the reduction potential at $E_{pc} = -1.35$ V continuously increased with increasing acid concentration (2–12 mM *p*-HOTs) with final cathodic shift of 290 mV indicating a catalytic proton reduction. The concerned cyclic voltammograms (Fig. 8) and unchanged electronic spectra (Fig. 9) on acid addition suggest an EC (electrochemical-chemical) mechanism as shown in Fig. 10.

Table 3
Crystal data and structural refinement for complexes **1**–**3**.

	1	**2**	**3**
Empirical formula	$C_{14}H_4Fe_2N_2O_6S_2$	$C_{27}H_{14}Fe_2N_2O_6S_2Cl_2$	$C_{12}H_2Fe_2N_2O_6S_3$
Formula weight	472.01	709.12	478.04
Temperature (K)	298 (2)	100 (2)	298 (2)
Crystal size (mm)	0.24 × 0.18 × 0.04	0.50 × 0.42 × 0.38	0.33 × 0.25 × 0.19
Crystal system	Monoclinic	Monoclinic	Monoclinic
Space group	$P2_1/c$	$C2/c$	$P2_1/c$
Z	4	8	4
Wavelength (Å)	0.71073	0.71073	0.71073
a [Å]	18.0645 (13)	36.976 (6)	22.247 (8)
b [Å]	6.8573 (5)	7.5657 (11)	6.877 (3)
c [Å]	13.2585 (10)	25.353 (4)	14.146 (5)
α (°)	90.0	90.0	90.0
β [°]	96.8580 (10)	124.119 (5)	94.152 (7)
γ (°)	90.0	90.0	90.0
Volume [$Å^3$]	1630.6 (2)	5871.8 (15)	2151.7 (14)
Calculated density (Mg/m^{-3})	1.923	1.604	1.472
Reflections collected/unique	6956/3139	23565/5175	19265/3741
R(int)	0.0228	0.0511	0.1160
F(000)	936	2848	944
Max. and min. transmission	0.9217 and0.6363	0.6268 and0.5504	0.7434 and 0.6105
Θ range for data collection (°)	1.14 to 25.98	1.33 to 25.06	1.84 to 24.98
Refinement method	Full-matrix Least-squares on F^2	Full-matrix Least-squares on F^2	Full-matrix Least-squares on F^2
Data/restraints/parameters	3139/0/235	5175/0/370	3741/0/226
Goodness-of-fit on F^2	1.053	1.069	1.037
R_1/wR_2 [I > 2sigma(I)]	0.0313/0.0764	0.0647/0.01567	0.0746/0.1559
R_1/wR_2 (all data)	0.0353/0.0785	0.0789/0.1655	0.1372/0.1782
Largest diff. peak and hole [$e.Å^{-3}$]	0.531 and-0.319	1.193 and-0.952	0.652 and −0.513

3. Conclusion

We have described the synthesis, characterization and electrochemistry of three *N*-heterocyclic cis-1,2 dithiolato bridged diiron complexes as potential models for the active sites of the [FeFe] hydrogenase. *N*-heterocyclic cis-1,2 dithiols belong to an important ligand system as far as the active sites of many metalloenzymes are concerned. Molybdopterin, a well characterized co-factor associated the active sites molybdenum hydroxylases, contains *N*-heterocyclic cis-1,2 dithiol as a ligand coordinated to the metal center and this class of enzymes catalyses many essential oxidation–reduction reactions. It was proposed that cis-1,2 dithiolato (non-innocent) ligand plays an important role in these redox/electron transfer reactions. The metallo-enzyme of the present context, [FeFe] hydrogenase is also known as an important redox enzyme catalyzing an acid to dihydrogen. Therefore, complexes that contains *N*-heterocyclic cis-1,2 dithiolato bridged diiron centers would serve as potential models for [FeFe] hydrogenases. Even through, the number of reports of modeling the active sites of iron only hydrogenases is not anymore limited, the number of diiron model systems that contains bridged *N*-heterocyclic cis-1,2 dithiolato ligand is very limited. All three model complexes **1**–**3**, reported in the present study, are *N*-heterocyclic cis-1,2 dithiolato bridged diiron complexes. Interestingly, each of the three carbonyl complexes **1**, **2** and **3** display one quasi–reversible two electron reduction at relatively very low potentials ($E_{1/2} = -1.23$, -1.24 and -1.25 V *vs*. Fc/Fc^+ for **1**, **2** and **3** respectively) compared to other related model compounds. We have demonstrated the electrocatalytic proton reduction of a strong acid *p*-toluenesulfonic acid mediated by compounds **2** and **3**. For the electrocatalytic proton reduction by the all-carbonyl compound [$Fe_2\{\mu$-diph-6,7-qdt$\}(CO)_6$] (**2**), we have proposed CEEC mechanism. The hexa carbonyl compound [$Fe_2\{\mu$-btdt$\}(CO)_6$] (**3**) does not undergo protonation with *p*-toluenesulfonic acid in its $\{Fe^IFe^I\}$ oxidation state, probably due to the involvement/delocalization of lone pair of electrons of ring nitrogen with ring sulfur pi-electrons. Accordingly an EC electrocatalytic reduction mechanism is proposed for compound **3**.

4. Experimental section

4.1. General procedures

All the reactions were carried out using standard Schlenk and vacuum-line technique under an atmosphere of nitrogen. Dichloromethane was distilled from CaH_2, THF from sodium/benzophenone ketyl, and MeOH, EtOH from Mg powder under a N_2 atmosphere. 1,2-diamino benzene (from Loba), $Fe_2(CO)_9$ and Me_3NO were purchased from Aldrich and directly used without further purification. Micro analytical (C, H, N) data were obtained with a FLASH EA 1112 series CHNS Analyzer. The IR spectra (with KBr pellet) were recorded in the range of 400–4000 cm^{-1} on a JASCO FT/IR-5300 spectrometer. Electronic spectra were obtained on a Cary 100 Bio UV–Visible spectrophotometer. ^1H, ^{13}C and $^{31}P\{^1H\}$ NMR spectra were recorded on Bruker DRX–400 spectrometer using $Si(CH_3)_4$ (TMS) as an internal standard. Solution mass spectra (LC–MS) were obtained on a LC–MS-2010A Shimadzu spectrometer. Melting points were measured in open capillary tubes and are uncorrected.

4.2. Single crystal structure determination of complexes 1–3

Single crystals suitable for facile structural determination for the compounds **1**, **2** and **3** were measured on a three circle Bruker SMART APEX CCD, area detector system under [λ (Mo Kα) = 0.7103 Å], graphite monochromator X-ray beam, 2400 frames were recorded with an ω scan width of 0.3°, each for 8 s, crystal-detector distance 60 mm, collimator 0.5 mm. Data reduction performed by SAINTPLUS [55]. Empirical absorption corrections using equivalent reflections performed program SADABS [55]. Absorption corrections using multi Ψ-scans were applied. The structures were solved by direct methods and least-square refinement on F^2 for all the compounds **1**–**3** by using SHELXS-97 [56]. All the non hydrogen atoms were refined anisotropically. Hydrogen atoms on the aromatic rings were introduced on calculated positions and included in the refinement riding on their respective parent atoms. The crystallographic parameters, data collection and structure refinement of the compounds **1**–**3** are summarized in Table 3.

4.3. Electrochemical studies of complexes 1–3

Acetonitrile (Finar, HPLC grade) used for performance of electrochemistry was dried with molecular sieve (4 Å) and then freshly distilled from CaH_2 under N_2. A solution of 0.1 M [nBu_4N][ClO_4] (TBAP) (Across, electrochemical grade) in CH_3CN was used as supporting electrolyte. Electrochemical measurements were recorded by using a BAS electrochemical analyzer. The electrolyte solution was degassed by bubbling with dry Argon for 10 min before measurement. Cyclic voltammograms were obtained in a three-electrode cell under argon. The working electrode was a glassy carbon disc (diameter 3 mm) successively polished with 0.3-μm alumina paste and sonicated in an ion–free water for 10 min; it was then washed with ethanol and finally rinsed with acetone followed by air drying before usage. The home-built reference electrode was a silver wire in contact with a solution of 0.1 M *n*–Bu_4NClO_4 and 0.01 M $AgNO_3$ in acetonitrile. The reference electrode was separated from the contents of the cell by means of a porous Vycor frit. When not in use, the reference electrode assembly was kept immersed in 0.1 M *n*–Bu_4NClO_4/acetonitrile to prevent drying of the frit. The auxiliary electrode was a platinum wire. The potentials, reported here, are quoted against the ferrocene/ferrocenium (Fc/Fc^+) couple.

4.3.1. Preparation of 2,3-Diphenyl-6,7-bis-thiocyanato-quinoxaline (B)

A mixture containing 1,2-diaminobenzene-bis(thiocyanate) (300 mg, 1.35 mmol), benzil (316 mg, 1.50 mmol) and iodine (10 mol%) in CH_3CN (10.0 mL) was stirred for 1 h. The resulting yellow precipitate was separated by filtration, washed with little CH_3CN, and dried in *vaccuo*. Yield: 0.45 g (84.0%); Yellow solid; LC–MS: $m/z = 395$ $[M - H]^+$. IR (KBr pellet, cm^{-1}): 3067(C–H Str, Ar), 2160 (C≡N str), 1653, 1597, 1537, 1435, 1390, 1338, 1253, 1194, 1057, 1022, 952, 893, 871, 769, 723, 698, 597, 543, 493. ^1H NMR (400 MHz, $CDCl_3$) δ: 8.66 (s, 2H), 7.55 (d, 4H), 7.36–7.46 (m, 6H) ppm. ^{13}C NMR ($CDCl_3$): δ 156.32, 141.47, 137.75, 134.35, 129.95, 129.88, 128.53, 126.72, 107.91 ppm. Anal. Calc. for $C_{22}H_{12}N_4S_2$: C, 66.64; H, 3.05; N, 14.13%. Found: C, 66.48; H, 3.14; N, 14.25%.

4.3.2. Preparation of 2,3-diphenyl-quinoxaline-6,7-dithiol (H_2diph-6,7-qdt)

2,3-diphenyl-6,7-bis-thiocyanato-quinoxaline (0.3 g, 0.757 mmol) was added as a solid to a solution of Na_2S (0.3 g, 3.85 mmol) in 100 mL of degassed water and the mixture was heated to 70–80 °C for 24 h to produce a clear, orange-red solution. The mixture was cooled to room temperature, and 20 mL of 10% HCl was added drop-wise to afford a heavy, brown precipitate. The precipitate was filtered off, washed with water, and air-dried. Thus dithiol ligand was obtained. Yield: 0.180 g (68.6%). LC–MS: $m/z = 347$ $[M - H]^+$. IR (KBr pellet, cm^{-1}): 3057 (C–H Str, Ar), 2530 (S–H str), 1581, 1533, 1433, 1388, 1338, 1253, 1188, 1059, 1022, 960, 869, 765, 727, 694, 596, 543. ^{13}C NMR (DMSO-d^6): δ 145.2, 140, 136.5, 134, 131.0, 129, 128.5, 127.0 ppm. Anal. Calc. for

$C_{20}H_{14}N_2S_2$: C, 69.33; H, 4.07; N, 8.09%. Found: C, 69.86; H, 3.92; N, 7.82%.

[Fe_2{μ-6,7-qdt}$(CO)_6$] (1). A mixture of $Fe_2(CO)_9$ (0.9 g, 2.474 mmol) and $H_2$6,7-qdt (0.48 g, 2.474 mmol) was refluxed in THF (25 mL) for 3 h to give a blood red solution containing some black solid in suspension. The mixture was filtered, and the solvent was removed under the reduced pressure, the residue was subjected to column chromatography by using hexane/CH_2Cl_2 (4:1 v/v) as eluents. The major red band was obtained as a red solid. Yield: 0.3 g (25.6% based on thiol). It was recrystallized by cooling at −10 °C. LC–MS: m/z = 473.0 $[M + H]^+$. IR (KBr pellet, cm^{-1}): 2945(m), 1541(m), 760(vs) $\nu_{(C\hat{}O)}$ 2072(s), 2028(s), 2008(s), 1993(s), 1973(s). ^{1}H NMR (400 MHz, $CDCl_3$) δ: 8.66 (s, 2H), 7.86 (s, 2H) ppm. ^{13}C NMR ($CDCl_3$, δ): 207.0, 148.3, 145.8, 142.0, 128.2 ppm. Anal. Calc. for $C_{14}H_4Fe_2N_2O_6S_2$: C, 35.62; H, 0.85; N, 5.93%. Found: C, 35.55; H, 0.87; N, 6.05%.

[Fe_2{μ-diph-6,7-qdt}$(CO)_6$] (2). A mixture of $Fe_2(CO)_9$ (0.902 g, 2.482 mmol) and H_2diph-6,7-qdt (0.860 g, 2.482 mmol) was refluxed in THF (25 mL) for 3 h and followed same procedure for the preparation of **1**. The residue was subjected to column chromatography by using hexane/CH_2Cl_2 (4:1 v/v) as eluents. It was recrystallized by cooling at −10 °C. Yield: 0.5 g, (33% based on thiol). IR (KBr pellet, cm^{-1}): 2950(m), 1550(m), 765(vs) $\nu_{(C\equiv O)}$ 2076(s), 2037(s), 2028(s), 2003(s), 1973(s). ^{1}H NMR (400 MHz, $CDCl_3$) δ: 7.94 (s, 2H), 7.43–7.29 (m, 10H) ppm. ^{13}C NMR ($CDCl_3$, δ): 207.0, 147.8, 140.07, 138.3, 129.6, 129.1, 128.3, 128.0 ppm. Anal. Calc. for $C_{26}H_{12}Fe_2N_2O_6S_2$: C, 50.03; H, 1.93; N, 4.48%. Found: C, 50.12; H, 2.05; N, 4.38%.

[Fe_2{μ-btdt}$(CO)_6$] (3). A mixture of $Fe_2(CO)_9$ (0.91 g, 2.5 mmol) and H_2btdt (0.5 g, 2.5 mmol) was refluxed in THF (25 mL) for 3 h and followed same procedure as discussed for the preparation of **1**. It was recrystallized by cooling at −10 °C. Yield: 0.3 g, (25.1% based on thiol). LC–MS: m/z = 479.3 $[M + H]^+$. IR (KBr pellet, cm^{-1}): 2964(m), 2928(m), 1649(m), 1506(m), 1425(m), 1261(m), 1095(m), 850(m), 760(vs), $\nu_{(C\equiv O)}$ 2075(s), 2038(s), 2007(s), 1983(s). ^{1}H NMR (400 MHz, $CDCl_3$) δ: 7.85 (s, 2H) ppm. ^{13}C NMR ($CDCl_3$, δ): 206.9, 153.7, 147.7, 120.2 ppm. Anal. Calc. for $C_{12}H_2Fe_2N_2O_6S_3$: C, 30.15; H, 0.42; N, 5.86%. Found: C, 30.21; H, 0.48; N, 5.76%.

4.3.3. Protonation experiment

5 mg of *p*-HOTs was added to a solution of complex **2** (10 mg) in CH_3CN (2 mL). The solution was stirred for 5 min. The red solution turned into dark red. This dark red solution was then subjected to FTIR studies. As expected, the IR spectrum exhibited significant changes in the carbonyl region (*vide supra*).

Acknowledgments

We thank Department of Science and Technology (DST), Government of India (Project No. SR/S1/IC–23/2007) and Centre for Nanotechnology at University of Hyderabad for financial support. The National X-ray Diffractometer facility at the University of Hyderabad by DST, Government of India, is gratefully acknowledged. We are grateful to UGC, New Delhi, for providing the infrastructure facility at University of Hyderabad under a UPE grant. GDP and RB are grateful to CSIR, Government of India, New Delhi, for their fellowships. Special thanks are due to Dr. V. Madhu for initiating dithiolene project in our laboratory. We would like to acknowledge Prof. S. Pal and his research group, School of Chemistry, University of Hyderabad and Prof. M. Ravikanth, Dr. M. Rajesh, Dr. Yedukondalu, Department of Chemistry, IIT Bombay for their support in cyclic voltammetric studies.

Appendix. Supplementary material

Supplementary data related to this article can be found online at doi:10.1016/j.jorganchem.2012.01.021.

References

[1] R. Cammack, Nature 397 (1999) 214–215.
[2] D.J. Evans, C.J. Pickett, Chem. Soc. Rev. 32 (2003) 268–275.
[3] M. Frey, ChemBio Chem. 3 (2002) 153–160.
[4] J.W. Peters, W.N. Lanzilotta, B.J. Lemon, L.C. Seefeldt, Science 282 (1998) 1853–1858.
[5] Y. Nicolet, C. Piras, P. Legrand, C.E. Hatchikian, J.C. Fontecilla- Camps, Strcture 7 (1999) 13–23.
[6] G.A.N. Felton, C.A. Mebi, B.J. Petro, A.K. Vannucci, D.H. Evans, R.S. Glass, D.L. Lichtenberger, J. Organomet. Chem. 694 (2009) 2681–2699.
[7] D.M. Heinekey, J. Organomet. Chem. 694 (2009) 2671–2680.
[8] C. Tard, C.J. Pickett, Chem. Rev. 109 (2009) 2245–2274.
[9] J.-F. Capon, F. Gloaguen, F.Y. Petillon, P. Schollhammer, J. Talarmin, C. R. Chim. 11 (2008) 842–851.
[10] J.-F. Capon, F. Gloaguen, F.Y. Petillon, P. Schollhammer, J. Talarmin, Coord. Chem. Rev. 253 (2009) 1476–1494.
[11] F. Gloaguen, J.D. Lawrence, M. Schmidt, S.R. Wilson, T.B. Rauchfuss, J. Am. Chem. Soc. 123 (2001) 12518–12527.
[12] E.J. Lyon, I.P. Georgakaki, J.H. Reibenspies, M.Y. Darensbourg, J. Am. Chem. Soc. 123 (2001) 3268–3278.
[13] J.D. Lawrence, H. Li, T.B. Rauchfuss, M. Benard, M.M. Rohmer, Angew. Chem. Int. Ed. 40 (2001) 1768–1771.
[14] J. Windhager, H. Görls, H. Petzold, G. Mloston, G. Linti, W. Weigand, Eur. J. Inorg. Chem. 28 (2007) 4462–4471.
[15] L.-C. Song, Z.Y. Yang, H.Z. Bian, Y. Liu, H.T. Wang, X.F. Liu, Q.M. Hu, Organometallics 24 (2005) 6126–6135.
[16] P. Li, M. Wang, C. He, G. Li, X. Liu, C. Chen, B. Akermark, L. Sun, Eur. J. Inorg. Chem. (2005) 2506–2513.
[17] J.F. Capon, S.E. Hassnaoui, P. Schollhammer, J. Talarmin, Organometallics 24 (2005) 2020–2022.
[18] J.W. Tye, J. Lee, H. Wang, R. Mejia-Rodriguez, J.H. Reibenspies, M.B. Hall, M.Y. Darensbourg, Inorg. Chem. 44 (2005) 5550–5552.
[19] L. Duan, M. Wang, P. Li, Y. Na, N. Wang, L. Sun, Dalton Trans. (2007) 1277–1283.
[20] F. Gloaguen, J.D. Lawrence, T.B. Rauchfuss, J. Am. Chem. Soc. 123 (2001) 9476–9477.
[21] F. Gloaguen, J.D. Lawrence, T.B. Rauchfuss, M. Benard, M.-M. Rohmer, Inorg. Chem. 41 (2002) 6573–6582.
[22] K.A. Justice, R.C. Linck, T.B. Rauchfuss, S.R. Wilson, J. Am. Chem. Soc. 126 (2004) 13214–13215.
[23] A.C. Boyke, T.B. Rauchfuss, S.R. Wilson, M.-M. Rohmer, M. Benard, J. Am. Chem. Soc. 126 (2004) 15151–15160.
[24] L.-C. Song, M.-Y. Tang, S.-Z. Mei, J.-H. Huang, Q.-M. Hu, Organometallics 26 (2007) 1575–1577.
[25] L.-C. Song, L.-X. Wang, M.-Y. Tang, C.-G. Li, H.-B. Song, Q.-M. Hu, Organometallics 28 (2009) 3834–3841.
[26] L.-C. Song, Z.Y. Yang, Y.J. Hua, H.T. Wang, Y. Liu, Q.M. Hu, Organometallics 26 (2007) 2106–2110.
[27] J. Chen, A.K. Vannucci, C.A. Mebi, N. Okumura, S.C. Borowski, M. Swenson, T. Lockett, D.H. Evans, R.S. Glass, D.L. Lichtenberger, Organometallics 29 (2010) 5330–5340.
[28] J.A. Cabeza, A. Martinez-Garcia, V. Riera, Organometallics 17 (1998) 1471–1477.
[29] M.M. Hasan, M.B. Hursthouse, S.E. Kabir, K.M. Abdul Malik, Polyhedron 20 (2001) 97–101.
[30] A.K. Vannucci, S. Wang, G.S. Nichol, D.L. Lichtenberger, D.H. Evans, R.S. Glass, Dalton Trans. 39 (2010) 3050–3056.
[31] J.F. Capon, F. Gloaguen, P. Schollhammer, J. Talarmin, J. Electroanal. Chem. 566 (2004) 241–247.
[32] G.A.N. Felton, A.K. Vannucci, J. Chen, L.T. Lockett, N. Okumura, B.J. Petro, U.I. Zakai, D.H. Evans, R.S. Glass, D.L. Lichtenberger, J. Am. Chem. Soc. 129 (2007) 12521–12530.
[33] G.A.N. Felton, A.K. Vannucci, N. Okumura, L.T. Lockett, D.H. Evans, R.S. Glass, D.L. Lichtenberger, Organometallics 27 (2008) 4671–4679.
[34] L. Schwartz, P.S. Singh, L. Eriksson, R. Lomoth, S. Ott, C. R. Chim. 11 (2008) 875–889.
[35] D. Streich, M. Karnahl, Y. Astuti, C.W. Cady, L. Hammarström, R. Lomoth, S. Ott, Eur. J. Inorg. Chem. (2011) 1106–1111.
[36] S. Ezzaher, A. Gogoll, C. Bruhn, S. Ott, Chem. Commun. 46 (2010) 5775–5777.
[37] D. Streich, Y. Astuti, M. Orlandi, L. Schwartz, R. Lomoth, L. Hamarström, S. Ott, Chem. Eur. J. 16 (2010) 60–63.
[38] L. Schwartz, L. Eriksson, R. Lomoth, F. Teixidor, C. Viñas, S. Ott, Dalton Trans. (2008) 2379–2381.
[39] A. Majumdar, J. Mitra, K. Pal, S. Sarkar, Inorg. Chem. 47 (2008) 5360–5364.
[40] A. Majumdar, K. Pal, S. Sarkar, J. Am. Chem. Soc. 128 (2006) 4196–4197.
[41] G. Durgaprasad, R. Bolligarla, S.K. Das, J. Organomet. Chem. 696 (2011) 3097–3105.
[42] R. Bolligarla, G. Durgaprasad, S.K. Das, Inorg. Chem. Commun. 14 (2011) 809–813.
[43] J.L. Brusso, O.P. Clements, R.C. Haddon, M.E. Itkis, A.A. Leitch, R.T. Oakley, R.W. Reed, J.F. Richardson, J. Am. Chem. Soc. 126 (2004) 8256–8265.
[44] S.V. More, M.N.V. Sastry, C.-C. Wang, C.-F. Yao, Tetrahedron Lett. 46 (2005) 6345–6348.
[45] R. Bolligarla, S.K. Das, Tetrahedron Lett. 52 (2011) 2496–2500.

[46] A.L. Cloirec, S.P. Best, S. Borg, S.C. Davies, D.J. Evans, D.L. Hughes, C.J. Pickett, Chem. Commun. (1999) 2285–2286.
[47] E.J. Lyon, I.P. Georgakaki, J.H. Reibenspies, M.Y. Darensbourg, Angew. Chem. Int. Ed. 38 (1999) 3178–3180.
[48] X. Zhao, I.P. Georgakaki, M.L. Miller, J.C. Yarbrough, M.Y. Darensbourg, J. Am. Chem. Soc. 123 (2001) 9710–9711.
[49] J.L. Nehring, D.M. Heinekey, Inorg. Chem. 42 (2003) 4288–4292.
[50] J.D. Lawrence, T.B. Rauchfuss, S.R. Wilson, Inorg. Chem. 41 (2002) 6193–6195.
[51] A. Bondi, J. Phy. Chem. 68 (1964) 441–451.
[52] J.F. Capon, F. Gloaguen, P. Schollhammer, J. Talarmin, J. Electroanal. Chem. 595 (2006) 47–52.
[53] G.-A.N. Felton, R.S. Glass, D.L. Lichtenberger, D.H. Evans, Inorg. Chem. 45 (2006) 9181–9184.
[54] T. Liu, M. Wang, Z. Shi, H. Cui, W. Dong, J. Chen, B. Akermark, L. Sun, Chem. Eur. J. 10 (2004) 4474–4479.
[55] Bruker, SADABS, SMART, SAINT and SHELXTL, Bruker AXS Inc., Madison, Wisconsin, USA, 2000.
[56] G.M. Sheldrick, Acta Crystallogr. Sect. A 64 (2008) 112–122.